Estimation of Photovoltaic System Reliability and Performance Metrics

Sairaj V. Dhople, *Student Member, IEEE,* and Alejandro D. Domínguez-García, *Member, IEEE*

***Abstract*—A framework to integrate reliability and performance analysis of grid-tied photovoltaic (PV) systems is formulated using Markov reward models (MRM). The framework allows the computation of performance metrics such as capacity and energy yield, and reliability metrics such as availability. The paper also provides an analytical method to compute the sensitivity of performance metrics to MRM-parameter variations. The approach to sensitivity analysis is demonstrated to be particularly useful to formulate optimal operational policies, e.g., repair strategies, as the impact of variations in model parameters on system performance can be rapidly evaluated. Case studies demonstrate several applications of the proposed framework, including analysis of residential and large utility-level installations, and emerging distributed inverter architectures.**

***Index Terms*—Reliability, Markov reward models, photovoltaics, generalized matrix inversion, sensitivity analysis.**

I. Introduction

THERE has been a rapid growth in the deployment of photovoltaic (PV) energy-conversion systems in recent years. According to a National Renewable Energy Laboratory report, the installed PV capacity in the U. S. increased by 43% from 0.77 GW to 1.1 GW in 2008 [1]. Aggressive projections indicate that this number could increase up to 24 GW by 2015 [2]. To ensure continued growth, it is imperative to address the high levelized cost of energy (LCOE) for PV systems. The LCOE is defined as the ratio of the present value of capital and operating costs to the energy yield over the system's lifetime and serves as a useful metric to gauge the competitiveness of different sources of energy [1]. According to [3], PV plants that begin operation in 2016 are expected to have an LCOE of 210 $/MWhr (by comparison, the LCOE for wind energy conversion systems and conventional coal-fired plants was 97 $/MWhr and 94.8 $/MWhr, respectively). In order to obtain PV system LCOE, it is necessary to calculate, among other things, net annual energy production, levelized operating and maintenance (O&M) expenses, and levelized replacement/overhaul costs. The LCOE is inversely proportional to the net annual energy production, and directly proportional to O&M and replacement/overhaul costs [1]. Therefore, system reliability has a great impact not only on O&M and replacement/overhaul costs, but also on annual energy yield. This dependence has been evidenced by studies that demonstrated that LCOE of PV sources increases exponentially with a decrease in lifetime [4].

System reliability/performance models should provide accurate energy-yield estimation, and aid in system design to ensure favorable economics. Additionally, an important aspect is the impact of model-parameter uncertainty, which will in turn propagate to the LCOE estimate. This paper addresses the problems discussed above by providing: i) a modeling framework to integrate reliability considerations into energy-yield and cost estimations using Markov Reward Model (MRM) formalisms [5]; and ii) an analytical approach for MRM parameter sensitivity analysis based on generalized matrix inversion techniques [6].

Markov reward models result from mapping every state of a Markov chain to an appropriately defined, real-valued quantity that defines a metric—*the reward*—for measuring system reliability/performance. The underlying Markov chain captures system failure and repair behavior as in a standard reliability model. The appropriate choice of rewards yields various metrics of interest. For instance, energy yield can be obtained by defining the reward as the energy produced per unit time. Similarly, choosing the reward as cost per unit time allows computation of monetary gain (for PV electricity sold to the grid), and O&M or replacement/overhaul costs (to recover from failed states). Finally, reliability-related metrics such as availability can be naturally obtained by setting to one the reward corresponding to states of the Markov chain in which the system is operational, and to zero otherwise. The proposed modeling framework can be utilized to understand the trade-offs between different repair policies and O&M and replacement/overhaul costs.

The literature on system-level probabilistic reliability analysis for power systems is very extensive (see, e.g., [7], [8], [9] and the references therein). Since the scope of this paper is on PV energy-conversion-system reliability analysis, we will focus the literature review on reliability modeling of renewable energy systems, and only discuss system-level references that are related to our work. Markov reliability models for wind-energy systems, and small hydro power plants are proposed in [10] and [11], respectively. In the context of PV systems, combinatorial-based methods for PV system reliability assessment have been attempted in [12], [13], but they do not yield insight into other performance metrics such as energy yield and are limited in scope and application. Reliability-oriented design approaches for off-grid, remote PV systems are explored in [14], where the authors use Markov reliability models among other methods. The idea to utilize Markov chains in PV-system reliability modeling was also proposed in [15]. Our work is related to the ideas presented in [16], where the authors develop a model to integrate economic aspects in power system reliability and apply the concepts to a two-transformer example. The Markovian framework proposed

S. V. Dhople and A. D. Domínguez-García are with the Department of Electrical Engineering, University of Illinois at Urbana-Champaign, Urbana, IL, 61801. e-mail: {sdhople2, aledan}@ILLINOIS.EDU.

in this paper goes beyond standard Markov reliability models which provide metrics such as availability and mean-time-to-failure, and provides performance-related metrics such as energy yield, although other metrics that, for example, include cost as in [16] can be easily defined.

The impact of parameter uncertainty on reliability and performance metrics is an important aspect of system reliability/performance analysis, because accurately determining parameters such as failure and repair rates is difficult. Apart from identifying model parameters that are likely to cause modeling errors, such analyses also aid in optimal system design [17], [18]. We propose an analytical method for parametric sensitivity analysis for MRM models. Our work extends ideas for sensitivity analysis in discrete-time Markov chains [19] that builds upon the theory of generalized matrix inversion [6]. The case studies highlight how sensitivity analysis can be used to formulate optimal maintenance policies, estimate the impact of parameter variations, and aid in optimizing PV economics. In the context of power systems, analytical approaches to parametric sensitivity analysis for reliability models have received rather limited attention. A common problem that has been studied is the effect of generator failure/repair rate uncertainty on reliability metrics such as loss of load expectation [18], [20], [21]. Essentially, each generator has two possible states (operational/failed) and is described by a two-state Markov-reliability model, for which it is easy to obtain analytical sensitivities of the stationary distributions. However, if multiple generators or multiple failure modes are considered in a single reliability model, analytical solutions to the sensitivities cannot be obtained easily. In [22], sensitivity analysis requiring repeated simulations determines the factors that have the most effect on the availability of spare transformers in distribution stations. In other fields, e.g., computer systems, there is some work on parameter sensitivity analysis for Markov reliability models. For example, in [17], sensitivity analysis for acyclic Markov chains based on uniformization is applied to the study of multiprocessor systems.

The remainder of this paper is organized as follows. Section II formulates Markov reward models for reliability and performance evaluation, and proposes a method to compute the stationary distribution of the MRM underlying Markov chain, and its sensitivity to model parameters variations. Case studies in Section III demonstrate how the proposed framework can be employed to formulate optimal repair strategies in residential and utility-scale installations, aid in system-level design, and predict the performance of emerging distributed PV system architectures. Concluding remarks are presented in Section IV.

II. Framework Formulation

This section establishes a framework for PV system reliability and performance evaluation using MRMs, and proposes an analytical method for quantifying the effect of parameter variations on the MRM solution. Additionally, several metrics to measure the performance of PV systems are defined.

A. MRMs for Reliability and Performance Evaluation

A MRM model consists of a Markov chain taking values in some finite set $\mathcal{S}$, and a reward function that maps each element of $\mathcal{S}$ into a real-valued quantity which captures some performance metric of interest. In the context of this work, the Markov chain describes system stochastic behavior due to failures and repairs. Additionally, it is assumed that the system is perfectly repairable [23], and thus the resulting Markov chain is ergodic, which essentially means that every state in the Markov chain is accessible from every other state [24].

Let $X = \{X(t), t \geq 0\}$ denote a Markov chain taking values in a finite set $\mathcal{S} = \{0, 1, 2, \ldots, n\}$, where $0, 1, 2, \ldots, n-1$ index PV system configurations that arise due to component faults, and n indexes the nominal, non-faulty configuration. Let $\pi_i(t)$, $t \geq 0$, be the probability that the system is in state i, and define the corresponding probability vector as $\pi(t) = [\pi_0(t), \pi_1(t), \ldots, \pi_n(t)]$. The evolution of $\pi(t)$ is defined by the Chapman-Kolmogorov equations

$$\dot{\pi}(t) = \pi(t)\Lambda, \tag{1}$$

with $\pi_n(0) = 1$, $\pi_j(0) = 0$, $j = 0, 1, \ldots, n-1$, and where Λ is the Markov-chain generator matrix. To determine the Markov-chain generator matrix, the first step is to list all possible states that arise from different component fault sequences. Transitions between states involve failures and repairs and are hence governed by a combination of failure and repair rates [23]. The Markov-chain generator matrix is given by $\Lambda = [\lambda_{ij}]$, where λ_{ij} is the rate at which the process makes a transition from state i to j, and $\lambda_{ii} = -\sum_{j \neq i} \lambda_{ij}$. While smaller models can be constructed manually, software packages can be used to model and analyze larger and more complicated systems [25], [26], [27].

Let $\varrho : \mathcal{S} \rightarrow \mathbb{R}$ be a *reward function* that maps each PV system configuration $i = 0, 1, 2, \ldots, n$ into a real-valued quantity ρ_i that quantifies system performance while in configuration i.

1) Performance Metrics Definition: At each time t, the values that the reward function ϱ takes can be described by a random variable $\mathcal{P}(t)$ with the same probability density function as $X(t)$, i.e., $\pi(t) = [\pi_0(t), \pi_1(t), \ldots, \pi_n(t)]$. Thus, a probabilistic measure of system performance at time t is given by the expected value of $\mathcal{P}(t)$:

$$\Xi(t) = \mathrm{E}[\mathcal{P}(t)] = \sum_{i=0}^{n} \rho_i \pi_i(t) = \pi(t) \cdot \rho', \tag{2}$$

where $\rho = [\rho_0, \rho_1, \ldots, \rho_n]$. A long-term measure of system performance is given by

$$\Xi = \mathrm{E}[\mathcal{P}] = \sum_{i=0}^{n} \rho_i \pi_i = \pi \cdot \rho', \tag{3}$$

where $\pi = [\pi_0, \pi_1, \ldots, \pi_n]$ is the Markov-chain stationary distribution. If the values that the reward function ϱ takes are defined in per-unit time, e.g., energy produced per unit time, then Ξ describes the average rate at which the system will deliver/consume some quantity that measures the system performance, e.g., energy production. Then, it is possible to obtain the accumulated quantity measuring system performance in

some period of time $[0,\, T]$, $T \gg t_0$ as

$$\Gamma = \int_0^T \mathrm{E}[\mathcal{P}(t)]dt = \int_0^T \pi(t) \cdot \rho' dt \approx \pi \cdot \rho' \cdot T, \qquad (4)$$

where t_0 is such that the effect of initial conditions in (1) has vanished. For example, if the entries in ρ are defined in units of power generated by the PV system, then Γ yields the expected energy yield in T units of time. A short note on the validity of the approximation in (4) is given in the Appendix.

2) Reliability/Performance Metrics of Interest: A wide variety of metrics can be defined by MRMs by appropriately formulating ϱ [5]. We provide a few examples of these performance/reliability metrics, some of which will be used in the PV system case studies discussed in Section III. In all these examples, it is assumed that the stochastic behavior due to component failures and repairs is described by an ergodic Markov chain, (i.e., the system is perfectly repaired) with states $i = 0,\, 1,\, 2, \ldots,\, n-1$ indexing system configurations that arise due to faults, and $i = n$ indexing the non-faulty configuration.

Expected System Capacity: Consider a PV system with power rating P. Denote by π_i the long-term probability that the system is operating in configuration i, and the corresponding power rating by P_i. The expected system capacity is denoted by Ξ, and following (3), it can be defined as

$$\Xi = \pi\rho' = [\pi_0\, \pi_1\, ...\pi_n]\, [P_0\, P_1\, ...P_n]'\,. \qquad (5)$$

Effectively, this metric ensures that PV systems with the same power rating but different reliability models can be uniformly and unambiguously compared.

Energy Yield: Consider a grid-tied PV system installed at a location characterized by a capacity factor CF which is defined as

$$CF = \frac{(\text{h/day of 1-sun})}{24\,\text{h/day}}, \qquad (6)$$

where 1-sun is defined as an insolation of 1 kW/m^2 [28]. For example, if the average incident PV energy density at a given location is 5 kWh/m^2-day, this corresponds to 5 h/day of 1-sun insolation, and a capacity factor of 20.8 %. Average capacity factors for different locations are computed using historical PV data and can be obtained from a variety of sources (see, e.g., [28]). Over some period of time T, if the system satisfies the conditions in (4), an estimate of its energy yield is given by

$$\Gamma = \Xi \cdot CF \cdot T. \qquad (7)$$

Multiplying the energy yield by the average price of electricity yields the monetary gain over the period T. In Section IV-A, we describe a method for explicitly considering uncertainty in the PV source and how it can be propagated to reliability and performance metrics. This method reformulates the entries of the reward vector as random variables whose distributions are derived from those of incident insolation and ambient temperature, the uncertain inputs to the PV system.

System Availability: By appropriate choice of the reward function, a MRM can also provide standard reliability metrics. For example, system availability for an $n+1$ state model can be recovered by choosing ρ so that $\rho_i = 1$ if the system is operational in state i and $\rho_i = 0$ otherwise.

B. Analytical Approach to Parametric Sensitivity Analysis

The stationary distribution of an ergodic Markov chain is a function of the generator matrix parameters. In the context of this work, the generator matrix parameters are the failure and repair rates, which are assumed to be not perfectly known. Let the elements in $\Theta = \{\theta_1,\, \theta_2, \ldots, \theta_m\}$ denote the parameters of the generator matrix, and define the corresponding parameter vector $\theta = [\theta_1,\, \theta_2, \ldots, \theta_m]$. Given the functional dependence of the generator matrix on θ, i.e., $\Lambda(\theta)$, we are interested in studying the functional dependence of the stationary distribution on θ, i.e., $\pi(\theta) = [\pi_1(\theta),\, \pi_2(\theta),\, \ldots \pi_n(\theta)]$.

For ergodic Markov chains, the generator-matrix group inverse enables the analytical calculation of $\partial\pi_i(\theta)/\partial\theta_j\ \forall i,\, j$. The group inverse $\Lambda^{\#}$ of $\Lambda = \Lambda(\theta)$, for some θ, is the unique solution of

$$\begin{cases} \Lambda\Lambda^{\#}\Lambda = \Lambda, \\ \Lambda^{\#}\Lambda\Lambda^{\#} = \Lambda^{\#}, \\ \Lambda\Lambda^{\#} = \Lambda^{\#}\Lambda, \end{cases} \qquad (8)$$

if and only if $rank(\Lambda) = rank(\Lambda^2)$. The sensitivity of the stationary distribution to the i parameter, θ_i, is given by

$$\frac{\partial\pi(\theta)}{\partial\theta_i} = -\pi(\theta)\frac{\partial\Lambda(\theta)}{\partial\theta_i}\Lambda^{\#}. \qquad (9)$$

The proof of (9) is included in the Appendix. The sensitivity of the performance metric Ξ to the i parameter θ_i can be obtained from (3) and (9) as

$$\frac{\partial\Xi}{\partial\theta_i} = \frac{\partial\pi(\theta)}{\partial\theta_i}\rho'. \qquad (10)$$

C. Numerical Computation of the Stationary Distribution and the Group Inverse

A number of techniques have been proposed to compute the group inverse [6]. An approach involving the QR factorization of Λ, yields π and $\Lambda^{\#}$ [19]. In this method, Λ is expressed as $\Lambda = QR$, where, $Q,\, R \in \mathbb{R}^{n+1\mathrm{x}n+1}$. The matrix R is of the form

$$R = \begin{bmatrix} U & -Ue' \\ 0 & 0 \end{bmatrix}, \qquad (11)$$

where $U \in \mathbb{R}^{nxn}$ is a nonsingular upper-triangular matrix, and $e \in \mathbb{R}^n$ is a row vector with all elements equal to one. The stationary distribution is obtained by normalizing the last column of $Q = [q_1,\, q_2, \ldots,\, q_{n+1}]$, i.e.,

$$\pi = \frac{q'_{n+1}}{\sum_{i=1}^{n+1} q_{i,n+1}}, \qquad (12)$$

The group inverse is related to Q and R as follows:

$$\Lambda^{\#} = (I - e'\pi)\begin{bmatrix} U^{-1} & 0 \\ 0 & 0 \end{bmatrix} Q^T (I - e'\pi). \qquad (13)$$

We illustrate the concepts presented in this section with a simple example.

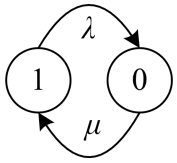

Figure 1. State-transition diagram for Example 1

Example 1. Consider a component with two possible operational states. In state 1, the component performs its intended function, and in state 0, it has failed. The failure rate of the component is denoted by λ, and the repair rate is denoted by μ. The state of the component (functional or failed) can be described by a two-state Markov chain. The state-transition diagram for this chain is illustrated in Fig. 1, from which it follows that the generator matrix is given by

$$\Lambda = \begin{bmatrix} -\mu & \mu \\ \lambda & -\lambda \end{bmatrix}. \tag{14}$$

The stationary distribution of the chain, $\pi = [\pi_0, \pi_1]$, obtained by solving $\pi \cdot \Lambda = 0$ with $\pi \cdot e' = 1$, where $e = [1\,1]$, is given by

$$\pi_0 = \frac{\lambda}{\mu+\lambda}, \quad \pi_1 = \frac{\mu}{\mu+\lambda}, \tag{15}$$

from which the following sensitivities can be derived

$$\frac{\partial \pi_0}{\partial \mu} = -\frac{\partial \pi_1}{\partial \mu} = -\frac{\lambda}{(\lambda+\mu)^2}, \tag{16}$$

$$\frac{\partial \pi_0}{\partial \lambda} = -\frac{\partial \pi_1}{\partial \lambda} = \frac{\mu}{(\lambda+\mu)^2}. \tag{17}$$

We will now verify that by using (9), the same result is obtained. The QR factorization of Λ is

$$Q = \frac{1}{\sqrt{\lambda^2+\mu^2}} \begin{bmatrix} -\mu & \lambda \\ \lambda & \mu \end{bmatrix}, \tag{18}$$

$$R = \begin{bmatrix} \sqrt{\lambda^2+\mu^2} & -\sqrt{\lambda^2+\mu^2} \\ 0 & 0 \end{bmatrix}. \tag{19}$$

As described in (12), the stationary distribution can be obtained by normalizing the last column of Q in (18). Comparing (19) and (11), we see that $U = \sqrt{\lambda^2+\mu^2}$. Substituting U, (15) and (18) in (13) yields

$$\Lambda^{\#} = \frac{1}{(\lambda+\mu)^2} \begin{bmatrix} -\mu & \mu \\ \lambda & -\lambda \end{bmatrix}. \tag{20}$$

The sensitivity of the stationary distribution to μ and λ can be derived from (9) as

$$\frac{\partial \pi}{\partial \mu} = -\pi \frac{\partial \Lambda}{\partial \mu} \Lambda^{\#} = \begin{bmatrix} -\frac{\lambda}{(\lambda+\mu)^2} & \frac{\lambda}{(\lambda+\mu)^2} \end{bmatrix} \tag{21}$$

$$\frac{\partial \pi}{\partial \lambda} = -\pi \frac{\partial \Lambda}{\partial \lambda} \Lambda^{\#} = \begin{bmatrix} \frac{\mu}{(\lambda+\mu)^2} & -\frac{\mu}{(\lambda+\mu)^2} \end{bmatrix} \tag{22}$$

where $\frac{\partial \Lambda}{\partial \mu} = \begin{bmatrix} -1 & 1 \\ 0 & 0 \end{bmatrix}$, $\frac{\partial \Lambda}{\partial \lambda} = \begin{bmatrix} 0 & 0 \\ 1 & -1 \end{bmatrix}$, $\pi = [\pi_0, \pi_1]$ is given by (15), and $\Lambda^{\#}$ is given by (20). Note that the sensitivities match those computed directly from the closed-form stationary distribution in (16)-(17). ■

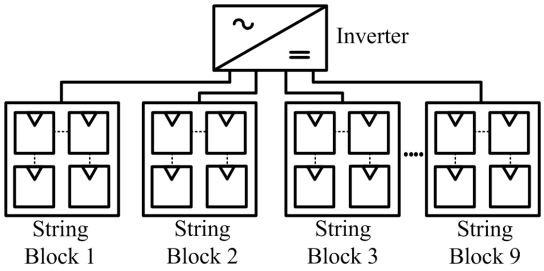

Figure 2. Block diagram of utility-scale system discussed in the case study.

III. Case Studies

The first case study applies to a utility-level system, and explores the impact of parameter variations and repair strategies on system capacity and energy yield. Next, sensitivity analysis is utilized to optimize repair rates for a residential-scale system. Finally, the sensitivity approach is utilized for design trade off analysis of emerging distributed PV architectures.

A. Utility-Scale Installations

Utility-owned installations constituted 8% of grid-tied PV systems in 2008 [29]. This number is expected to increase as federal legislation has incentivized utilities to own PV projects without separate tax investors [1]. The average installed capacity in utility installations is typically in the range of hundreds of kilowatts. While economies of scale guarantee lower operation and maintenance (O&M) costs (0.12% as compared to 1.47% for residential systems according to [1]), the large size and complexity of these systems presents various challenges to ensure high reliability.

The benchmark installation considered here is a P =225 kW grid-tied inverter analyzed in [30]. The system architecture is depicted in Fig. 2, where it can be seen that the inverter has nine string blocks (with rated power, $P_s = P/9 = 25$kW), each of which consist of ten strings of series-connected PV modules. Each string has twelve series-connected modules. In this case study, we assume there are two different failure modes: inverter and string blocks failures, with failure rates denoted by λ_i and λ_s, respectively. The inverter and string blocks are repairable with repair rates denoted by μ_i and μ_s, respectively, and repair brings the system back to its full functionality (although alternate repair strategies are explored subsequently). The state-transition diagram for the system stochastic behavior due to failures and repairs is depicted in Fig. 4. Note that other failure mechanisms including: failures in series strings (e.g. due to arc faults), individual PV modules (e.g. due to faulty junction boxes or bypass diodes), blocking diodes, and protection equipment, can be incorporated in the model by appropriately defining additional states. If appropriate transition rates can be identified, phenomena such as soiling and partial shading can also be modeled similarly.

1) Base Case: The performance metrics of interest are system capacity Ξ, and energy yield Γ. Following the notation in (5), it follows that $\rho_i = P_i = (i-1)P_s = (i-1)P/9$, $i = 1, ..., 10$, and $\rho_0 = 0$ (this configuration corresponds to inverter failure, which takes the whole system down at

once). The failure and repair rate values for the base case are $\lambda_i = (1/3)\ \text{yr}^{-1}$, $\lambda_s = (1/270)\ \text{yr}^{-1}$, $\mu_i = (365/15)\ \text{yr}^{-1}$, and $\mu_s = (365/8)\ \text{yr}^{-1}$ which are adopted from [30]. The system capacity is Ξ = 221.94 kW. Then, assuming a capacity factor, $CF = 18\%$, and for a period $T = 10$ yr, an estimate of the energy yield is $\Gamma = 3.51$ GWhr.

2) Failure/Repair Rate Uncertainty Analysis: Given the uncertainty in accurately determining transition rates [4], sensitivity analysis can reveal what parameters have the largest impact on system capacity (and therefore energy yield). Figures 3 (a)-(d) depict the system capacity sensitivity with respect to transition rates. Notice that system capacity is most sensitive to the inverter failure rate, followed by the string failure rate, inverter repair rate, and string repair rate. This follows intuitively as a failure in the inverter brings the system down, whereas the system still delivers power if several strings have failed. Also, note that $\partial\Xi/\partial\mu_s$ and $\partial\Xi/\partial\mu_i$ vary by over two orders of magnitude over the range of μ_s and μ_i, respectively. This suggests that accurate estimates of repair rates (or at least an accurate estimate on their range) are required for any analysis that employs sensitivity analysis. To validate the accuracy of the analytical results on sensitivity, we plot on the same figures the sensitivities computed numerically ($\partial\Xi/\partial\theta_i \approx \Delta\Xi/\Delta\theta_i$) which are seen to match those computed using the analytical approach very well.

3) Impact of Repair Strategy on Repair Costs: Denote by n_s, the largest number of operational strings for which repair is initiated. Figure 5 depicts the investigated repair strategies as n_s is varied from 8 to 1. Transitions due to inverter failure still exist but are not depicted in the figure for simplicity. The energy yield is calculated using (7) for the different repair strategies over a period of T =10 yr and capacity factor 18%. The results are plotted in Fig. 6. As expected, if more strings are allowed to fail before repair is initiated, the expected energy yield is reduced. Energy-yield estimates can be used to determine an alternative to the perfect repair

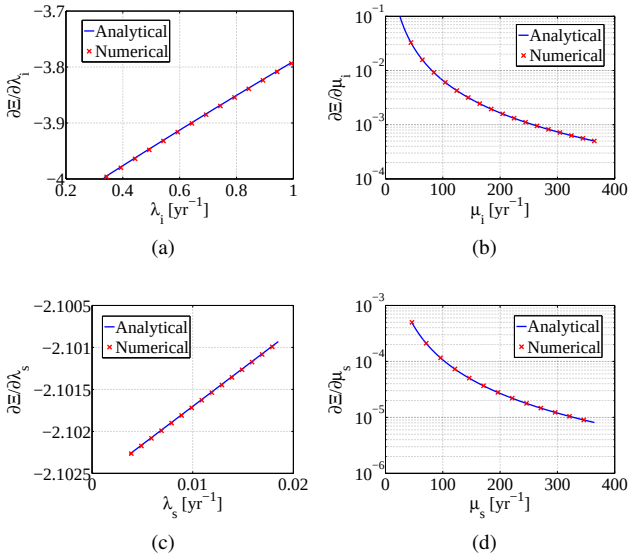

Figure 3. Capacity sensitivity as a function of transition rates

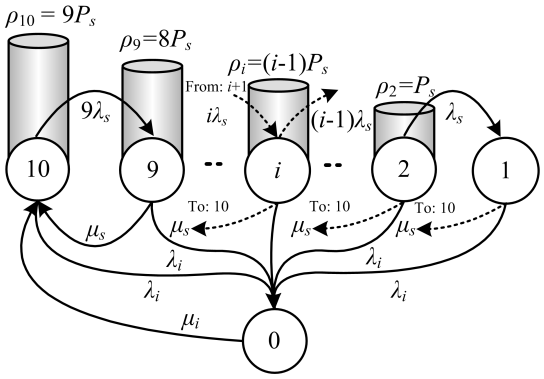

Figure 4. State-transition diagram for utility-scale installation

strategy (corresponding to $n_s = 8$). To do so, we introduce the marginal utility of repair for the j repair strategy which is denoted by MUR_j and defined as

$$MUR_j = \frac{p(\Gamma_8 - \Gamma_j)}{CF \cdot T} \frac{\$}{\text{yr}}, \tag{23}$$

where Γ_j is the energy yield in kWhr when $n_s = j$, p is the price of electricity in \$/kWhr. Essentially the marginal utility of repair suggests the added dollar amount by which the cost of the repair strategy when $n_s = j$ can be relaxed with no monetary loss to the system operator. Hence, one way to pick a repair strategy (or pick an n_s) given an added repair cost c_r \$/yr over the perfect repair strategy, is to solve the optimization problem

$$\begin{aligned} &\text{Maximize} \quad j \\ &\text{Such that} \quad c_r < MUR_j \\ &\qquad\qquad 1 \le j \le 8. \end{aligned} \tag{24}$$

The MUR for the example above is plotted in Fig. 7 assuming that the price of electricity is 8.7 cents/kW-hr. For the illustrative repair cost (denoted by c_r and sketched as a dashed line in the figure), we would pick the repair strategy corresponding to $n_s = 6$.

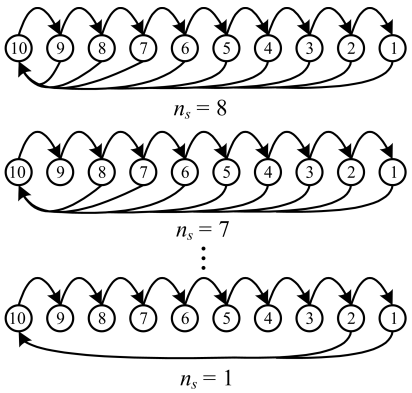

Figure 5. Alternate repair strategies

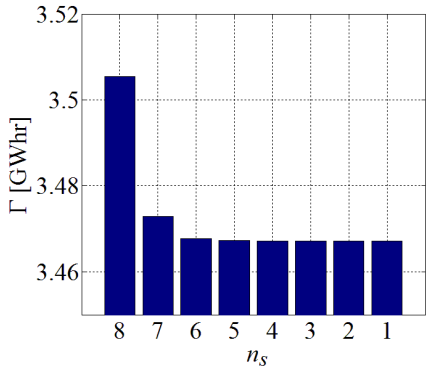

Figure 6. Energy yield as a function of repair strategy

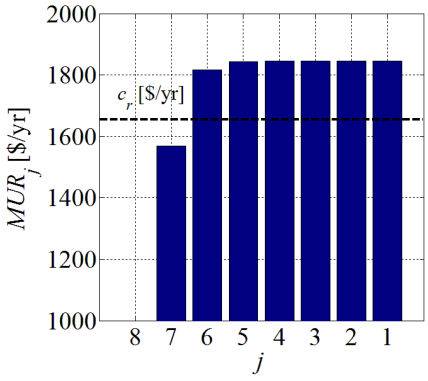

Figure 7. Marginal utility of repair utilized to pick repair strategy

B. Optimum Repair Strategies for Residential PV Systems

Residential-scale systems had an average rating of 4.9 kW and constituted 27% of all new grid-connected systems installed in 2008 [29]. While traditionally such systems have been installed and operated by the homeowner, utilities have started to enter this sector. For example, San Diego Gas and Electric owns multi-family residential-scale PV systems, and Southern California Edison has similar initiatives to deploy utility-owned PV systems [2]. To encourage growth in this sector, technical advances have to be coupled with improvements in economics. Focusing on this aspect, this case study demonstrates how the proposed framework—especially the approach to sensitivity analysis—can optimize repair rates for residential-scale systems.

The benchmark PV installation studied here is installed in the Gable Home—a net-zero solar-powered home constructed by the University of Illinois for the 2009 Solar Decathlon Competition [31]. The system is comprised of a 9 kW PV array with forty 225 W modules. Two 5 kW inverters are utilized to interface with the utility grid. A block diagram of the system architecture is shown in Fig. 8. The PV system could operate (albeit at a lower power rating) with a single inverter should one fail. The Markov model developed to study this system focuses on inverter reliability as inverter failure has been singled out as one of the chief reasons for low energy yield in grid-connected PV systems [32]. Figure 9 depicts the Markov-model state-transition diagram that captures inverter

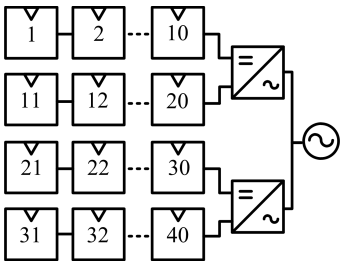

Figure 8. Gable Home electrical system block diagram

failures and repairs. Each state in the diagram represents the number of functional inverters. The failure rate of the inverters is denoted by λ. The repair rates corresponding to state 0 (the failed state) and state 1 (single functional inverter) are denoted by μ_0 and μ_1, respectively. This model captures the possibility that the time taken to repair two inverters could be longer than that to repair a single inverter. From the above description, it follows that $\rho = [\rho_0\ \rho_1\ \rho_2] = [0\ P/2\ P]$, $P = 10$ kW.

To demonstrate how repair rates might be chosen, let us begin by assuming that the mean time to inverter failure is $10\,\mathrm{yr}$ ($\lambda = (1/10)\ \mathrm{yr}^{-1}$) [1]. Assume that the mean time to repair the inverters is $10\,\mathrm{days}$ ($\mu_0 = \mu_1 = (365/10)\ \mathrm{yr}^{-1}$). The sensitivities of the system capacity to the failure and repair rates are: $\partial\Xi/\partial\lambda = -2.724\mathrm{x}10^{-2}$, $\partial\Xi/\partial\mu_1 = 7.424\mathrm{x}10^{-5}$, and $\partial\Xi/\partial\mu_0 = 4.068\mathrm{x}10^{-7}$. From these numbers it is clear that Ξ is not sensitive to the mean time to repair both inverters. This makes intuitive sense, as the inverters are very reliable and restored to operation rather quickly. These observations suggest that μ_0 need not equal μ_1. The quantities $\partial\Xi/\partial\mu_0$ and Ξ are plotted in Fig. 10 as a function of μ_0. The capacity is normalized as $\Xi = \Xi \cdot (100/P)$ to express it in %. Notice that the performance of the system is unaffected as long as the mean time to repair both inverters is between 10 and 30 days (corresponds to μ_0 between $36.5\,\mathrm{yr}^{-1}$ and $12.16\,\mathrm{yr}^{-1}$). This suggests that the mean time to repair two inverters could be relaxed to 30 days without affecting the energy yield.

Similar case studies can provide invaluable insight to manufacturers and installers in determining replacement, repair, and shipment policies to minimize costs. On the other hand, system owners can not only compare the performance of several different systems with a unified performance metric but also negotiate power purchase agreements, warranties and

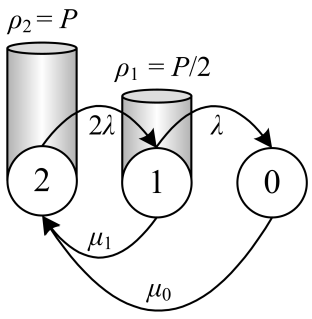

Figure 9. State-transition diagram capturing Gable Home inverter reliability.

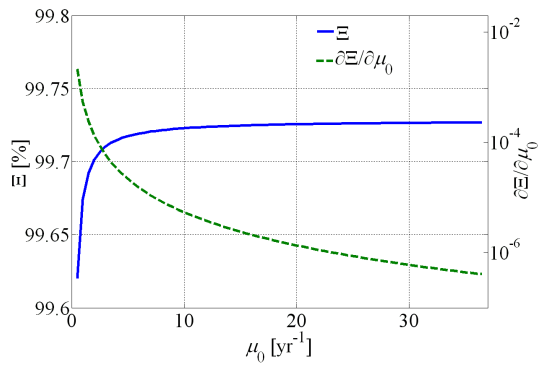

Figure 10. System capacity and its sensitivity to time to repair both inverters.

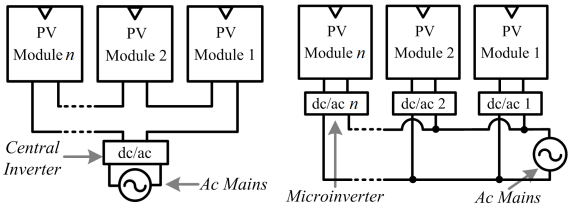

Figure 11. Block diagrams of the (a) central and (b) distributed inverter architectures.

repair policies. With proper data, the models can easily be extended to include a detailed economic analysis by coupling the repair rates with shipping and wage-related costs.

C. Emerging Distributed Inverter Systems

Conventional installations where large PV arrays were connected to central inverters (Fig. 11(a)) are expected to be replaced by distributed systems in which PV modules are coupled with module-integrated microinverters (Fig. 11(b)). Proponents of such systems have touted various advantages to justify the added installed cost over central systems [33]. Of particular interest is the reliability of microinverter-based architectures. The main goals of this case study are to evaluate the impact of failure and repair rates on system capacity.

Consider a grid-tied PV system built with n microinverters. The state-transition diagram for this system is shown in Fig. 12. As before, each state corresponds to the number of operational microinverters. Repairs in each state are assumed to restore the operation of all failed microinverters. The mean time to repair the microinverters is denoted by μ, and their failure rate is denoted by λ. Such a repair model is reasonable if the shipping time (which is ideally independent of the number of microinverters) is greater than the time taken to replace the faulty units. The stationary distribution for this chain is

$$\pi_0 = \left[1 + \sum_{i=1}^{n} \left(\prod_{k=1}^{i} \frac{\mu + (k-1)\lambda}{k\lambda} \right) \right]^{-1}, \qquad (25)$$

$$\pi_i = \frac{\mu + (i-1)\lambda}{i\lambda} \pi_{i-1} \quad \forall\, 1 \leq i \leq n. \qquad (26)$$

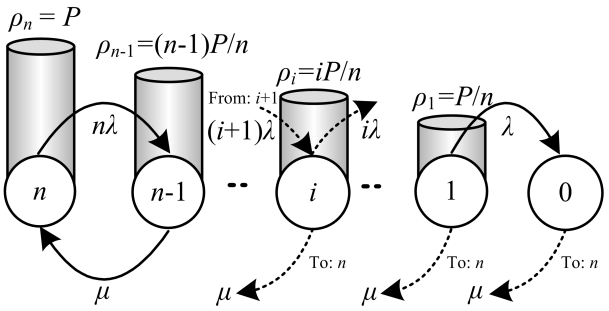

Figure 12. State-transition diagram for an n-microinverter PV system.

For a system rated at P W comprising n microinverters, the reward vector and system capacity are given by

$$\rho = [\rho_0\, \rho_1 \ldots \rho_i \ldots \rho_n] = \left[0\, \frac{P}{n} \ldots \frac{iP}{n} \ldots P\right], \qquad (27)$$

$$\Xi = \sum_{i=1}^{n} \rho_i \cdot \pi_i = \sum_{i=1}^{n} \frac{i}{n} \cdot P \cdot \pi_i, \qquad (28)$$

where the stationary distribution follows from (25)-(26). In light of the complicated expressions above, the utility of the proposed numerical method in computing the stationary distribution and its sensitivity to variations in system parameters is immediately obvious.

1) Performance Metrics Variation with Number of Inverters: We evaluate the relationship between the number of inverters, n, and the system capacity Ξ. Figure 13 depicts the system capacity as a function of the number of microinverters for three cases. In case 1, λ and μ are assumed to be the same as the base values, $\lambda = 1/10\,\mathrm{yr}^{-1}$ and $\mu = 365/10\,\mathrm{yr}^{-1}$, for all n. In case 2, λ is fixed to the base value, while μ is varied as shown in Fig. 14. In case 3, μ is fixed to the base value, while λ is varied as shown in Fig. 14. The monotonic reduction in λ captures possible circuit-level reliability improvements, while the monotonic increase in μ aims to quantify better repair policies. It emerges that with invariant failure and repair rates, Ξ is not a function of the number of microinverters, n. Improvements can only be made by reducing the failure rates or increasing the repair rates.

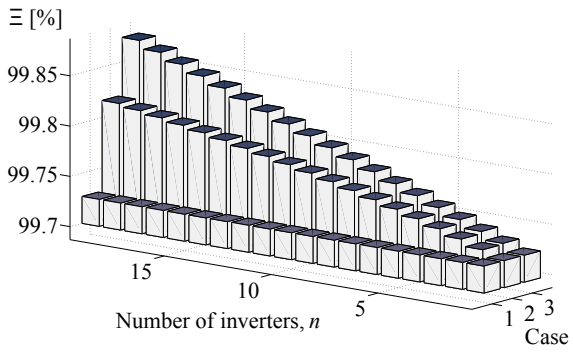

Figure 13. System capacity as a function of number of inverters.

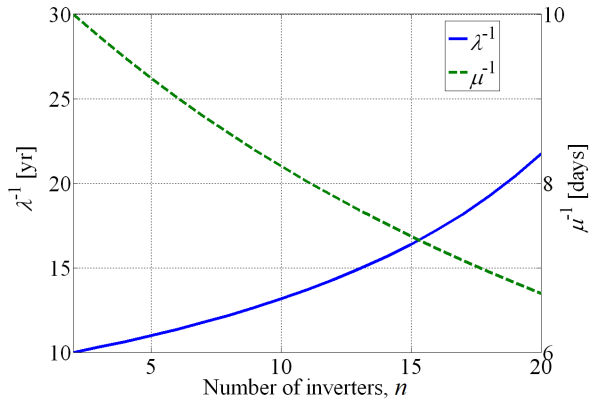

Figure 14. Illustrative failure and repair rates as a function of number of inverters adopted for case study.

2) Application of Sensitivity Analysis to System Design: Consider the design of a grid-tied 5 kW PV array to be implemented with microinverters. Suppose the system is built with twenty module-integrated microinverters. System capacity is plotted as a function of λ and μ in Fig. 15. A particularly useful application of the sensitivity analysis is to suggest necessary failure and repair rates to meet a specified performance requirement. To the first order, the sensitivity formulation implies that

$$\Delta\Xi \approx \frac{\partial \Xi}{\partial \theta}\Delta\theta' = \left[\frac{\partial \Xi}{\partial \theta_1}\ \frac{\partial \Xi}{\partial \theta_2}\cdots\frac{\partial \Xi}{\partial \theta_m}\right][\Delta\theta_1\ \Delta\theta_2\ \ldots\Delta\theta_m]'. \tag{29}$$

For instance, a performance change due to variations in failure rate can be estimated through

$$\Xi_1 \approx \Xi_0 + \frac{\partial \Xi}{\partial \lambda}(\lambda_1 - \lambda_0), \tag{30}$$

where variables subscripted by 0 are the nominal values. Referring to the 5 kW system considered above, it was noted that $\lambda_0 = 1/10\,\mathrm{yr}^{-1}$ and $\mu_0 = 365/10\,\mathrm{yr}^{-1}$, yielded $\Xi_0 = 99.73\%$. Suppose this were to be improved to $\Xi_1 = 99.90\%$ (with the same repair rate), (30) suggests that the required failure rate, $\lambda_1 = 1/26.667\,\mathrm{yr}^{-1}$. This can be verified numerically by calculating Ξ through (5).

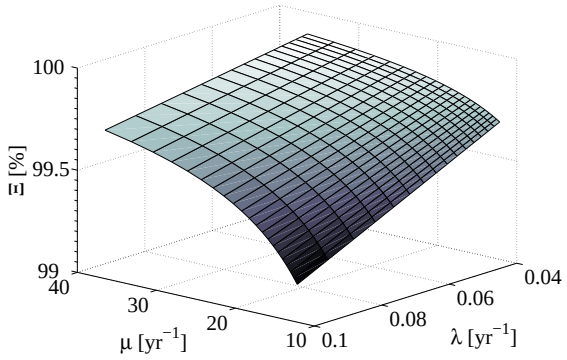

Figure 15. System capacity as a function of failure and repair rates for a microinverter system.

IV. Extensions and Future Work

In this section, we propose extensions to this work and provide an insight into possible avenues for future work.

A. Propagation of PV Source Uncertainty to Reliability and Performance Metrics

The power produced by the PV system is uncertain primarily because the incident insolation and ambient temperature—the inputs that determine the PV power output—are uncertain. As an alternative to the energy-yield estimation approach presented in Section II-A2 (which implicitly addressed uncertainty through the capacity factor), this section explores an explicit method to propagate input uncertainty to reliability metrics and PV energy-yield estimates. The first step is to reformulate the reward vector $\rho = [\rho_0, \rho_1, \ldots, \rho_n]$ as $R = [R_0, R_1, \ldots R_n]$, where R_i, $i = 0, 1, \ldots n$, are random variables. Then, we seek the mapping

$$R_i = f_i(S, \Delta), \tag{31}$$

where S and Δ are also random variables describing the incident insolation and ambient temperature at the given location. The function f_i captures the PV-system output in the i state and it can be formulated from standard PV performance models (see, e.g., [34]). Subsequently, system capacity, $\Xi = \pi \cdot R'$, and energy yield, $\Gamma = \Xi \cdot T$ are also random variables. The probability density functions (pdfs) of S and Δ, $f_S(s)$ and $f_\Delta(\delta)$ can be determined from field data or from analytical models. Then, the pdfs of the reward vector, system capacity, and energy yield, ($f_R(\rho)$, $f_\Xi(\xi)$, and $f_\Gamma(\gamma)$, respectively) can be determined through the method of transformation of random variables (see e.g., [24]).

B. Consideration of Extenuating Distribution-System Conditions and Common-Cause Failures

PV inverters are designed to meet the IEEE 1547 standard, which prescribes active power curtailment in case there are sustained over-voltage, under-voltage, over-frequency, or under-frequency conditions in the distribution system. The Markov reward modeling framework can be easily extended to accommodate these phenomena as described next. Consider Fig. 16, which depicts a three-state example (similar to the one presented in Section III-B of the manuscript) augmented with an additional state 0_F in which the power output is curtailed due to the extenuating phenomena described above. The power output is ρ_i in state i, ρ_j in state j and zero in state 0_F and state 0—which corresponds to the state in which no power is produced due to component failures. Transitions between the states i, j and state 0_F are introduced at the rates λ_F and μ_F, which can be determined from statistics of field data. As in the models described in the case studies, transitions between the states i, j and state 0 are due to component failure and repair (governed by transition rates λ_i, λ_j, and μ). Finally, catastrophic failures that cause the entire system to fail (e.g., failure in protection equipment, simultaneous failure in multiple inverters) can be modeled by introducing common-cause failures at the rate λ_C. Now,

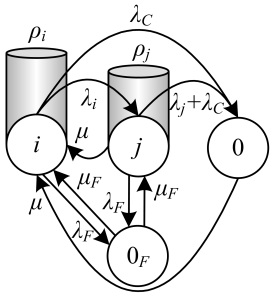

Figure 16. Addressing common-cause failures and under/over voltage/frequency conditions.

the system capacity $\Xi = \pi \cdot \rho' = \pi_i\rho_i + \pi_j\rho_j$ factors in the probability of over/under voltage/frequency conditions that cause active power curtailment, as well as common-cause failures.

V. Concluding Remarks

A Markov-reward-model based framework to evaluate PV-system reliability and performance has been formulated. Tools from generalized matrix inversion were utilized to derive the stationary distributions of the underlying Markov chains and their sensitivity to model parameters. Case studies demonstrated how the proposed framework can be utilized to drive system-level reliability and performance improvements. Future extensions can incorporate phenomena such as partial shading by introducing additional states in the Markov model and include capital and operational expenditure into the framework.

Appendix

A. Derivation of Result in (4)

The integral over which the accumulated reward is computed can be broken into two parts as

$$\Gamma = \int_0^T \pi(t)\cdot\rho' dt = \int_0^{t_0} \pi(t)\cdot\rho' dt + \int_{t_0}^T \pi\cdot\rho' dt, \qquad (32)$$

where t_0 is such that the effect of initial conditions in (1) has vanished. For $t \geq t_0$, the transition probability vector $\pi(t) = \pi$, the stationary distribution π. Applying the mean-value theorem [35], the above integral can be expressed as

$$\Gamma = \int_0^{t_0} \bar{\pi}\cdot\rho' dt + \int_{t_0}^T \pi\cdot\rho' dt = \bar{\pi}\cdot\rho'\cdot t_0 + \pi\cdot\rho'\cdot(T-t_0), \quad (33)$$

where $\bar{\pi} = \pi(t)|_{t=\tau}$ for some $\tau \in [0,\, t_0]$. If $T \gg t_0$, the second term in (22) dominates, and as a result,

$$\Gamma \approx \pi\cdot\rho'\cdot T \qquad (34)$$

B. Derivation of Result in (9)

The result in (9) follows from a similar theorem for discrete-time ergodic Markov chains presented in [19]. Theorem 3.2 in [19] considers an n-state, finite, homogeneous, ergodic Markov chain with transition matrix $P(\theta)$ and stationary distribution p. The sensitivity of the stationary distribution is given by

$$\frac{\partial p(\theta)}{\partial\theta_i} = -p(\theta)\frac{\partial A(\theta)}{\partial\theta_i}A^{\#}, \qquad (35)$$

where $A = I - P$, and $A^{\#}$ is the group inverse of A. As this work is concerned with continuous-time Markov chains, the result in [19] can not be applied directly to establish (9), because the matrix $I - \Lambda$ is not row stochastic. We will prove (9) by demonstrating that the stationary distribution of the underlying discrete-time Markov chain (DTMC) associated with the CTMC satisfies (35). Then, because the limiting behaviors of the DTMC and CTMC should match, (9) would follow. Consider that the CTMC is associated with a DTMC whose distribution is governed by

$$p[k+1] = p[k]P, \qquad (36)$$

where $P = I + \delta\Lambda$ is a row-stochastic, irreducible, and primitive matrix (with an appropriate choice of δ). Define the matrix $A = I - P = -\delta\Lambda$. The group inverse of Λ is denoted by $\Lambda^{\#}$, and given by

$$\Lambda^{\#} = -\delta A^{\#}. \qquad (37)$$

This can be shown by noting that $\Lambda^{\#}$ satisfies the definition of the group inverse given in (8). As the stationary solution of the DTMC and CTMC is the same, and

$$\frac{\partial\Lambda(\theta)}{\partial\theta_i}\Lambda^{\#} = \left(-\delta^{-1}\frac{\partial A(\theta)}{\partial\theta_i}\right)\left(-\delta A^{\#}\right) = \frac{\partial A(\theta)}{\partial\theta_i}A^{\#}, \quad (38)$$

the result in (9) follows from (35). Existence of the group inverse can be verified quite easily. Since the DTMC is assumed to be ergodic, the Perron-Frobenius theorem implies that 1 is a simple eigenvalue of P. Consequently, 0 is a simple eigenvalue of Λ and the Jordan form of Λ can be expressed as

$$\mathcal{J}_\Lambda = \begin{bmatrix} 0 & 0 \\ 0 & B \end{bmatrix}, \qquad (39)$$

where $B \in \mathbb{R}^{n-1\text{x}n-1}$ is non-singular. It immediately follows that $rank(\Lambda) = rank(\Lambda^2)$, which proves the existence of the group inverse [36].

References

[1] S. Price and R. Margolis, "2008 Solar Technologies Market Report," National Renewable Energy Laboratory, Tech. Rep., January 2010.

[2] T. Key, "Distributed Photovoltaics: Utility Integration Issues and Opportunities," Electric Power Research Institute, Tech. Rep., August 2010.

[3] "Levelized Cost of New Generation Resources in the Annual Energy Outlook 2011," Energy Information Administration, Tech. Rep., March 2011.

[4] J. E. Granata and M. A. Quintana, "System Level Reliability Methodologies," Sandia National Laboratories, Tech. Rep., July 2009.

[5] R. A. Sahner, K. S. Trivedi, and A. Puliafito, *Performance and Reliability Analysis of Computer Systems*. Norwell, MA: Kluwer Academic Publishers, 2002.

[6] S. L. Campbell and C. D. Meyer Jr., *Generalized Inverses of Linear Transformations*. Mineola, NY: Dover Publications, 1991.

[7] G. Anders, *Probability Concepts in Electric Power Systems*. New York, NY: John Wiley & Sons, 1990.

[8] R. Billinton and R. Allan, *Reliability Assessment of Large Power Systems*. Boston, MA: Kluwer Academic Publishers, 1988.

[9] J. Endrenyi, *Reliability Modeling in Electric Power Systems*. Chichester, England: John Wiley & Sons, 1978.

[10] A. P. Leite, C. L. T. Borges, and D. M. Falcão, "Probabilistic wind farms generation model for reliability studies applied to brazilian sites," *IEEE Transactions on Power Systems*, vol. 21, no. 4, pp. 1493–1501, November 2008.

[11] C. L. T. Borges and R. J. Pinto, "Small Hydro Power Plants Energy Availability Modeling for Generation Reliability Evaluation," *IEEE Transactions on Power Systems*, vol. 23, no. 3, pp. 1125–1135, August 2008.

[12] M. A. Hamdy, M. E. Beshir, and S. E. Elmasry, "Reliability Analysis of Photovoltaic Systems," *Applied Energy*, vol. 33, no. 4, pp. 253–263, 1989.

[13] W. M. Rohouma, I. M. Molokhia, and A. Esuri, "Comparative Study of Different PV Modules Configuration Reliability," *Desalination*, vol. 209, pp. 122–128, April 2007.

[14] H. A. M. Maghraby, M. H. Shwehdi, and G. K. Al-Bassam, "Probabilistic assessment of photovoltaic generation systems," *IEEE Transactions on Power Systems*, vol. 17, no. 1, pp. 205–208, February 2002.

[15] L. H. Stember, W. R. Huss, and M. S. Bridgman, "A methodology for photovoltaic system reliability and economic analysis," *IEEE Transactions on Reliability*, vol. R-31, no. 3, pp. 296–303, August 1982.

[16] G. J. Anders and A. M. L. da Silva, "Cost Related Reliability Measures for Power System Equipment," *IEEE Transactions on Power Systems*, vol. 15, no. 2, pp. 654–660, May 2000.

[17] J. T. Blake, A. L. Reibman, and K. S. Trivedi, "Sensitivity Analysis of Reliability and Performability Measures for Multiprocessor Systems," in *Proceedings of the ACM Sigmetrics*, 1988, pp. 177–186.

[18] A. C. G. Melo and M. V. F. Pereira, "Sensitivity analysis of reliability indices with respect to equipment failure and repair rates," *IEEE Transactions on Power Systems*, vol. 10, no. 2, pp. 1014–1021, May 1995.

[19] G. H. Golub and C. D. Meyer Jr., "Using the QR Factorization and Group Inversion to Compute, Differentiate, and Estimate the Sensitivity of Stationary Probabilities for Markov Chains," *SIAM*, vol. 7, no. 2, pp. 273–281, April 1986.

[20] A. M. Oliveira, A. C. G. Melo, and L. M. V. G. Pinto, "Consideration of Equipment Failure Parameter Uncertainties in Bus Composite Reliability Indices," in *IEEE Power Engineering Society Winter Meeting*, 1999, pp. 448–453.

[21] A. D. Patton and N. H. Tram, "Sensitivity of generation reliability indices to generator parameter variations," *IEEE Transactions on Power Apparatus and Systems*, vol. PAS-97, no. 4, pp. 1337–1343, July 1978.

[22] G. A. Hamoud, "Assessment of Spare Transformer Requirements for Distribution Systems," *IEEE Transactions on Power Systems*, vol. 26, no. 1, pp. 174–180, February 2011.

[23] M. Rausand and A. Høyland, *System Reliability Theory*. Hoboken, NJ: Wiley Interscience, 2004.

[24] G. Grimmett and D. Stirzaker, *Probability and Random Processes*. Oxford University Press, 1992.

[25] R. Geist and K. S. Trivedi, "Reliability Estimation of Fault-Tolerant System: Tools and Techniques," *Computer*, vol. 23, no. 7, pp. 52–61, July 1990.

[26] A. D. Domínguez-García, "An Integrated Methodology for the Performance and Reliability Evaluation of Fault-Tolerant Systems," Ph.D. dissertation, Massachusetts Institute of Technology, Cambridge, MA, June 2007.

[27] P. S. Babcock IV, G. Rosch, and J. J. Zinchuk, "An Automated Environment for Optimizing Fault-Tolerant Systems Designs," in *Proc. Annual Reliability and Maintainability Symposium*, 1991, pp. 360–367.

[28] G. M. Masters, *Renewable and Efficient Electric Power Systems*. Hoboken, NJ: Wiley Interscience, 2004.

[29] L. Sherwood, "U. S. Solar Market Trends 2008," Interstate Renewable Energy Council, Tech. Rep., July 2009.

[30] J. S. Stein and S. P. Miller, "Stochastic PV Performance/Reliability Model," Sandia National Laboratories, Tech. Rep., April 2010.

[31] S. V. Dhople, J. L. Ehlmann, C. J. Murray, S. T. Cady, and P. L. Chapman, "Engineering systems in the gable home: A passive, net-zero, solar-powered house for the U. S. Department of Energy's 2009 Solar Decathlon," in *Proc. Power and Energy Conference at Illinois*, 2010, pp. 58–62.

[32] H. Laukamp, "Reliability Study of Grid-Connected PV Systems," International Energy Agency, Tech. Rep., March 2002.

[33] S. B. Kjaer, J. K. Pedersen, and F. Blaabjerg, "A Review of Single-Phase Grid-Connected Inverters for Photovoltaic Modules," *IEEE Transactions on Industry Applications*, vol. 41, no. 5, pp. 1292–1306, September/October 2005.

[34] D. L. King, W. E. Boyson, and J. A. Kratochvil, "Photovoltaic Array Performance Model," Sandia National Laboratories, Tech. Rep., Augustl 2004.

[35] H. K. Khalil, *Nonlinear Systems*. Upper Saddle River, NJ: Prentice Hall, 2002.

[36] C. D. Meyer Jr., "The Role of the Group Generalized Inverse in the Theory of Finite Markov Chains," *SIAM*, vol. 17, no. 3, pp. 443–464, July 1975.